Oral Diseases (2008) 14, 457–464. doi:10.1111/j.1601-0825.2007.01401.x

http://www.blackwellmunksgaard.com

ORIGINAL ARTICLE

Bone formation in rat calvaria ceases within a limited period regardless of completion of defect repair

T Honma[1,2], T Itagaki[1,2], M Nakamura[2], S Kamakura[3], I Takahashi[4], S Echigo[1], Y Sasano[2]

[1]*Division of Oral Surgery, Tohoku University Graduate School of Dentistry, Sendai, Japan;* [2]*Division of Craniofacial Development and Regeneration, Tohoku University Graduate School of Dentistry, Sendai, Japan;* [3]*Division of Clinical Cell Therapy, Department of Translational Research, Center for Translational and Advanced Animal Research (CTAAR), Tohoku University School of Medicine, Seiryo-Machi, Aoba-Ku, Sendai, Japan;* [4]*Division of Orthodontic and Dentofacial Orthopedics, Tohoku University Graduate School of Dentistry, Sendai, Japan*

A bone defect that is not repaired with bone completely is designated a non-union defect or a critical-size defect. The biological mechanism that regulates the process of bone repair of the critical-size defect remains unknown. The present study was designed to investigate bone repair in a critical-size defect compared with that in a smaller or non-critical-size defect. Our original standardized rat calvarial bone defect model was used for the experiment. The rate of bone formation was examined with X-ray morphometry and the bone production of osteoblasts and osteocytes was assessed by molecular histology with *in situ* hybridization for type I collagen and osteocalcin. Formation of repaired bone ceased within 24 weeks in both critical- and non-critical-size defects i.e. regardless of completion of the defect repair. The results suggested that osteoblasts and osteocytes cease bone formation, and the differentiation of osteoblast progenitors declines in 24 weeks. Also, bone repair proceeds from the periosteum on both sides of the parietal bone but not from the surface of the bony edge around the original defect. The results could provide useful information for clinical research on bone repair.

Oral Diseases (2008) **14**, 457–464

Keywords: bone defects; bone repair; osteoblasts; osteocytes; X-ray morphometry; type I collagen; osteocalcin; *in situ* hybridization

Introduction

There have been few reports on healing of bone defects, although some studies have investigated repair of bone fracture (Precious and Hall, 1994; Dimitriou *et al*, 2005; Einhorn, 2005). Promoting bone regeneration in defects generated in operations for tumours or cysts and tooth extraction has been an important issue clinically (Petite *et al*, 2000; Alsberg *et al*, 2001).

It has been suggested that the repair of bone defects depends on the size of the defect, i.e. a bone defect larger than a certain size (a critical size) cannot be healed with bone. The remaining defect is filled with fibrous connective tissues (Schmitz and Hollinger, 1986; Schmitz *et al*, 1990). It has not been known why a small defect can be repaired but a large defect cannot. Furthermore, little information is available on how bone formation ceases during the repair of a critical-size defect. Various studies have investigated the repair of critical-size bone defects with growth factors, biomaterials, cell and/or tissue implantation or any combination of those (Kamakura *et al*, 1999; Kamakura *et al*, 2001, 2002, 2004, 2006; Lutolf *et al*, 2003; Cowan *et al*, 2004), although the biological mechanism that regulates the healing of bone defects has not been fully understood. To pursue these issues, our study was designed to investigate the process of bone regeneration in large defects compared with those in small defects by examining the rate of bone formation with X-ray morphometry and assessing production of osteoblasts and osteocytes by molecular histology with *in situ* hybridization (ISH).

Materials and methods

Animals

Twelve-week-old male Wistar rats weighing from 260 to 280 g were used. They were obtained from the SLC Corporation (Kotoh, Shizuoka, Japan) and kept under a standard light–dark schedule and standard relative humidity. Stock diet and tap water were available *ad libitum*. All procedures were approved by the Animal Research Committee of Tohoku University (Kamakura *et al*, 1999).

Correspondence: Yasuyuki Sasano, DDS, PhD, Division of Craniofacial Development and Regeneration, Tohoku University Graduate School of Dentistry, Sendai 980-8575, Japan. Tel: +81 22 717 8285, Fax: +81 22 717 8288, E-mail: sasano@anat.dent.tohoku.ac.jp
Received 5 March 2007; revised 11 April 2007; accepted 19 April 2007

Table 1 The number of specimens used for quantitative radiograph analysis

	W1	*W2*	*W3*	*W4*	*W6*	*W12*	*W18*	*W24*	*W36*
3.8 mm Defect	4	4	4	4	3	4	0	3	0
8.8 mm Defect	4	4	5	5	8	10	3	3	3

Experimental procedures

The experimental rats were anaesthetized with intraperitoneal sodium pentobarbital (5 mg/100 g of body weight) supplemented by ether inhalation. An aseptic elliptical skin incision about 15 mm long was made along the bilateral temporal line. An identical incision was made on the periosteum and the flap was gently turned over. The calvarial bone was exposed through flapping the skin and the periosteum. A full-thickness standardized trephine defect, 3.8 or 8.8 mm in diameter, was made in the parietal bone under continuous saline buffer irrigation. Extreme care was exercised to avoid injury to the midsagittal blood sinus and dura mater. The periosteal and skin flaps were returned and sutured (Kamakura *et al*, 1999, 2001). Ninety-four rats were used, of which 45 had 8.8 mm defects and 26 had 3.8 mm defects (Table 1), which were examined by both X-ray morphometry and ISH, and the other 23 without any defect were controls for ISH.

The rats were anaesthetized with sodium pentobarbital (5 mg/100 g) supplemented by ether inhalation, and perfused through the aorta with 4% paraformaldehyde with 0.5% glutaraldehyde in 0.1 M phosphate buffer, pH 7.4, in weeks 1, 2, 3, 4, 6, 12, 18, 24 or 36 after the defects were made. Calvaria were removed and kept in the same fixative overnight at 4°C.

Quantitative radiographic analysis

The calvaria were radiographed by means of a microradiography unit (Softex CMR Unit; Softex, Tokyo, Japan) with X-ray film (FR; Fuji photo film, Tokyo, Japan) under standardized conditions (20 kV, 5 mA and 1 min). The radiographed films were scanned at 300 dots per inch in a flatbed scanner (GT-X800, Seiko Epson Corp., Suwa, Japan) equipped with a transparency adapter and a scanning software (Epson Scan, version 2.61, Seiko Epson Corp.). Radiopacity within the defect was quantified two-dimensionally on a computer (Windows® XP) equipped with version 0.4.0.2 Scion Image (Scion Corp. Frederick, MD, USA). The percentage of radiopacity within the trephination defect was calculated as the radiopaque area in the defect/area of the defect $\times$ 100 (Blanquaert *et al*, 1995). All data are expressed as mean $\pm$ SD. The statistical significance was assessed with Scheffé's *F*-test.

Tissue preparation

The fixed specimens were decalcified in autoclaved 10% EDTA in 0.01 M phosphate buffer, pH 7.4, for 4–6 weeks at 4°C. After dehydration through a graded series of ethanol solutions, the tissues were embedded in paraffin. Serial sections 5 μm thick were cut, and selected sections were processed for haematoxylin–eosin (H-E) staining or ISH.

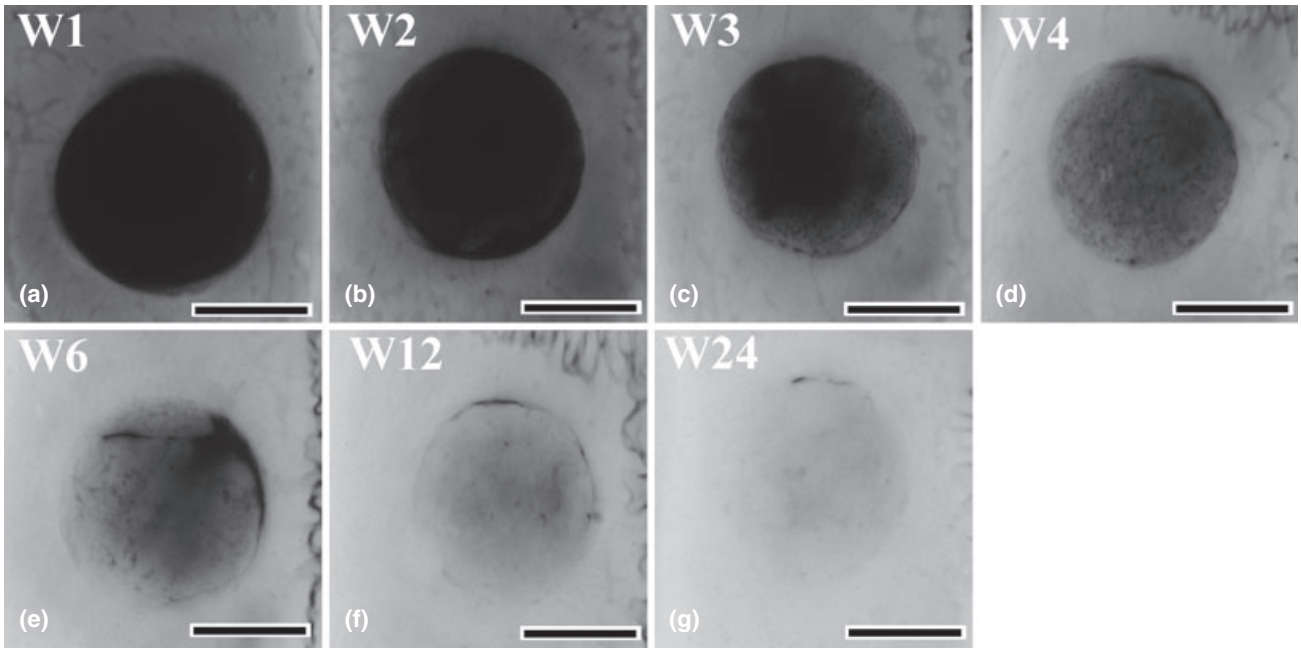

Figure 1 Radiographs of bone repair in 3.8 mm defects in weeks (W) 1 (**a**), 2 (**b**), 3 (**c**), 4 (**d**), 6 (**e**), 12 (**f**) and 24 (**g**). The defect is almost repaired with bone in 24 weeks. Scale bars = 2.2 mm

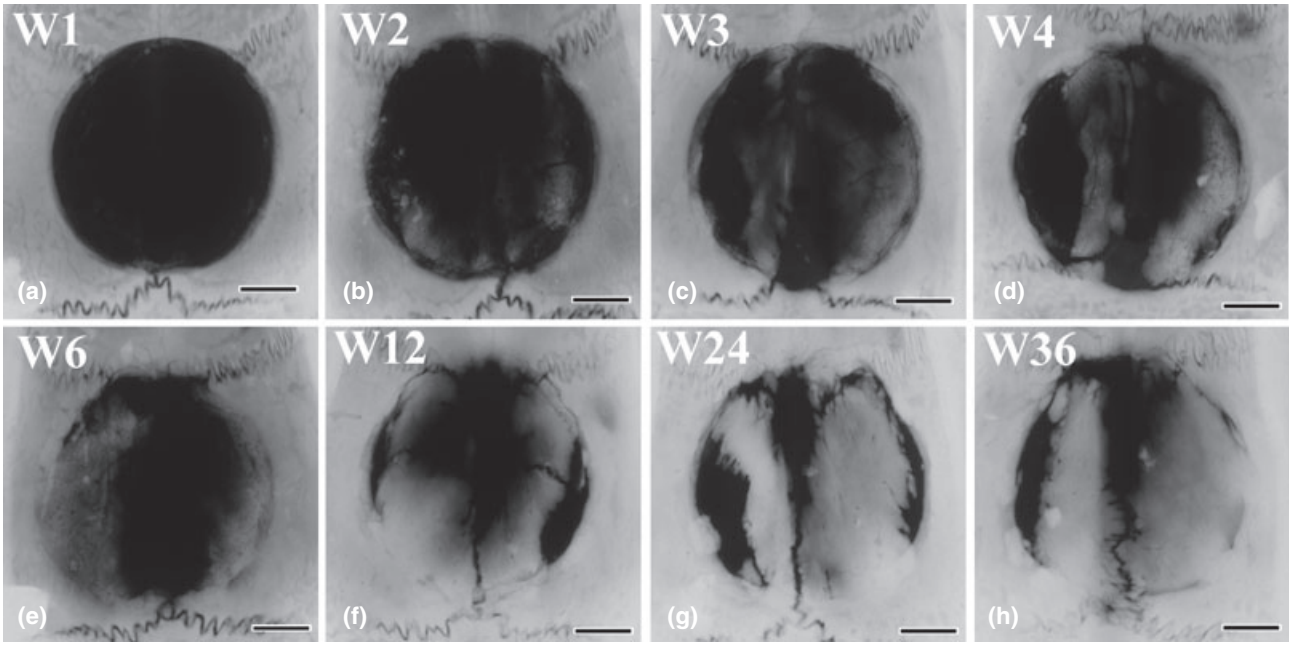

Figure 2 Radiographs of bone repair in 8.8 mm defects in weeks (W) 1 (**a**), 2 (**b**), 3 (**c**), 4 (**d**), 6 (**e**), 12 (**f**), 24 (**g**) and 36 (**h**). The defect is not completely repaired with bone in week 36. Scale bars = 2.2 mm

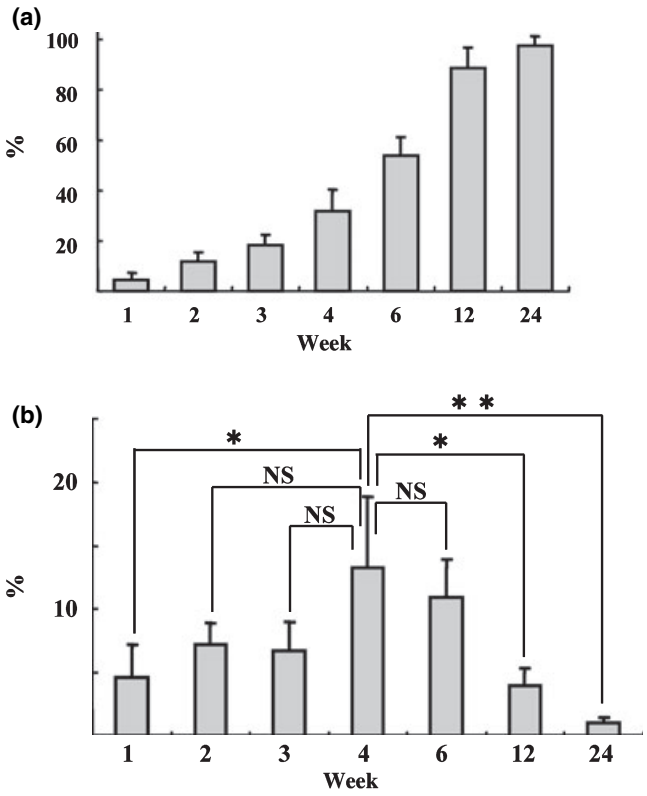

Figure 3 (**a**) Quantitative radiographic analysis for the total bone repair in the 3.8 mm defect. Bone repair proceeds gradually and is almost completed in week 24. (**b**) Quantitative radiographic analysis for bone repair per week in the 3.8 mm defect. The amount of repaired bone formation is the largest around the fourth week and decreases thereafter. Little bone is formed in the 24th week. Significance as compared with week 4, by a Scheffé's *F*-test, is indicated: $^{**}P < 0.01$, $^{*}P < 0.05$ and NS, not significant

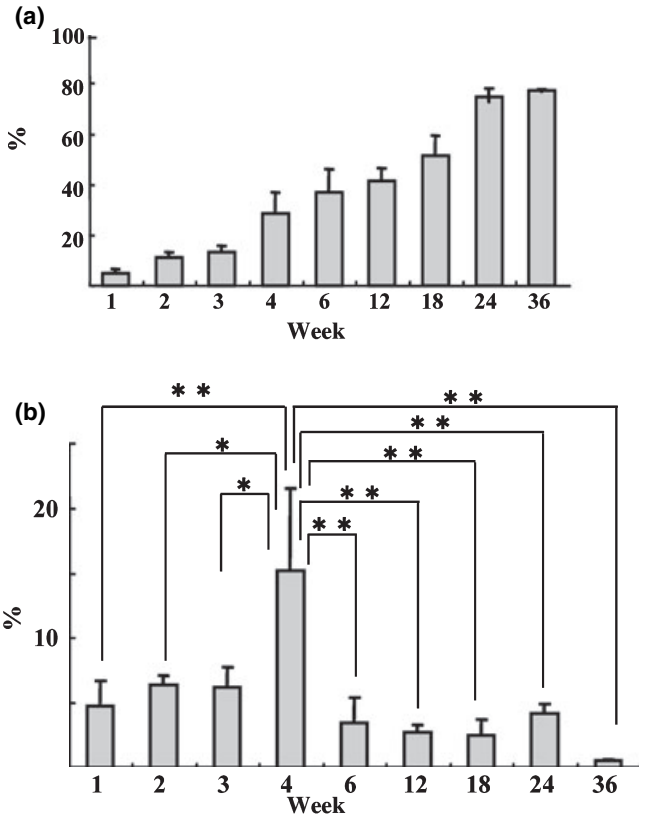

Figure 4 (**a**) Quantitative radiographic analysis for the total bone repair in the 8.8 mm defect. Bone repair proceeds gradually and almost ceases in week 24 with about 25% of the defect unrepaired. (**b**) Quantitative radiographic analysis for bone repair per week in the 8.8 mm defect. The amount of the bone repair is the largest in the fourth week and decreases thereafter. Little repaired bone formation is identified in the 36th week. Significance as compared to week 4, by a Scheffé's *F*-test, is indicated: $^{**}P < 0.01$, $^{*}P < 0.05$

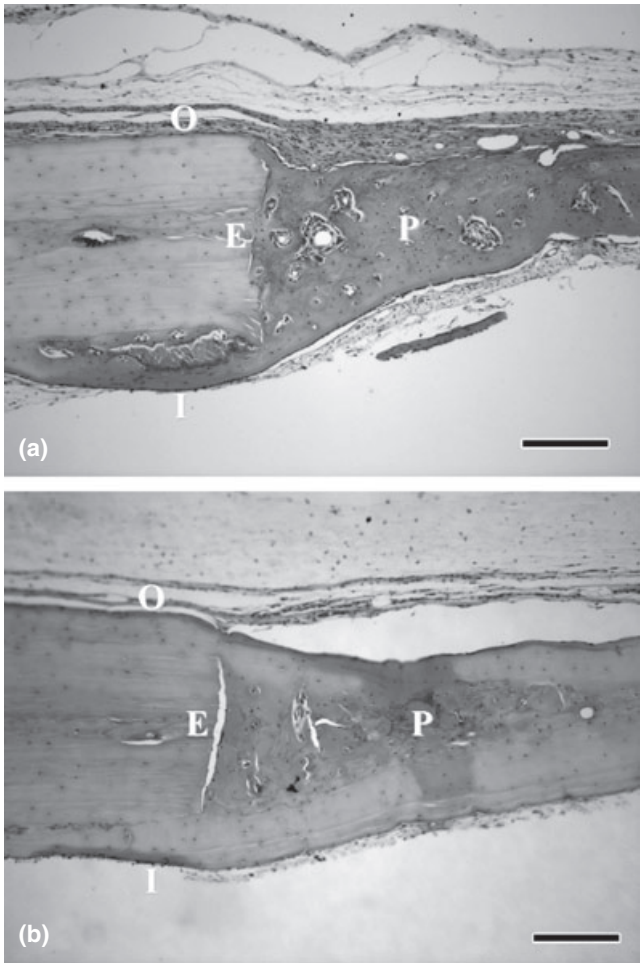

Figure 5 Haematoxylin–eosin staining of bone repair in 3.8 mm defects. Bone is formed in the defect from the outer (O) and inner (I) surfaces of the parietal bone in week 3 (**a**) and makes up the projection (P). The bone formation is more noticeable on the inner surface. The defect is filled with the bone projection in week 24 (**b**). E, the edge of the original defect. Scale bars = 200 μm

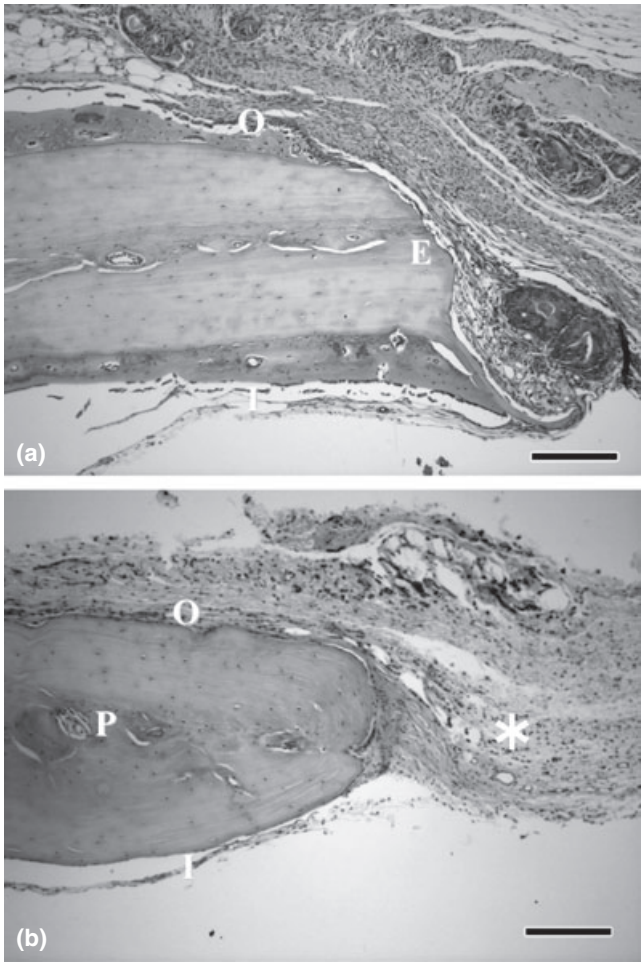

Figure 6 Haematoxylin–eosin staining of bone repair in 8.8 mm defects. Bone is formed in the defect from the outer (O) and inner (I) surfaces of the parietal bone in week 2 (**a**). The defect is not completely filled with bone and the unrepaired region is left with fibrous connective tissues (asterisk) in week 24 (**b**). E, the edge of the original defect; P, the bone projection. Scale bars = 200 μm

In situ *hybridization*

The protocol has been reported elsewhere (Nakamura *et al*, 2005) and is briefly described as follows:

The sections were deparaffinized and washed in phosphate-buffered saline (PBS), pH 7.4, and then immersed in 0.2 N HCl for 20 min. After being washed in PBS, the sections were incubated in proteinase K (20 g ml^{-1}; Roche; Mannheim, Germany) in PBS for 30 min at 37°C. After washing, the sections were dipped in 100% ethanol, dried in air and incubated with the antisense probe or the sense control probe (400 ng ml^{-1}) in a hybridization mixture for 16 h at 45°C. Digoxigenin-labelled, single-strand riboprobes for rat pro-alpha 1 (I) collagen (Sasano *et al*, 2002) and rat osteocalcin (Sasano *et al*, 2001) were used.

The sections were washed and treated with RNase (type 1A, 20 μg ml^{-1}; Sigma, St. Louis, MO, USA) for 30 min at 37°C. After washing, the hybridized probes were detected immunologically by using the Nucleic Acid Detection Kit (Roche), counterstained with methyl green, and mounted with a mounting medium.

At least two sections from each of three specimens at each stage were examined using the same probe. The intensity of hybridization signals was evaluated by observing at least three fields of every section.

Results

X-ray radiographs

X-ray radiographs showed that the 3.8 mm defect was almost filled with radiopaque bone in week 24 (Figure 1), while the 8.8 mm defect was not completely repaired by bone: some radiolucent regions were left in week 24 and even in week 36 (Figure 2).

Quantitative radiograph analysis

Defects 3.8 mm in diameter

Bone repair proceeded gradually and was almost complete in week 24 (Figure 3a). The amount of bone formation per week was the largest around the fourth week and decreased thereafter (Figure 3b). Little bone was formed in the 24th week.

Defects 8.8 mm in diameter
Bone repair proceeded gradually and almost ceased in week 24 with about 25% of the defect unrepaired (Figure 4a). The amount of bone repair per week was the largest in the fourth week and decreased thereafter (Figure 4b). Little bone was formed in the 36th week.

Histology
Defects 3.8 mm in diameter
Bone was formed in the defect from the outer surface, i.e. the parietal bone surface toward the skin and the inner surface fronted by the dura mater of the parietal bone near the edge around the defect in weeks 2 and 3 (Figure 5a). The bone formation was more noticeable on the inner surface than the outer surface. The repaired bone was lined by cuboidal osteoblasts. The defect was filled with the bone projection in week 24 (Figure 5b) and the repaired bone was lined by bone lining cells.

Defects 8.8 mm in diameter
Bone was formed in the defect from the outer bone surface toward the skin and the inner or dural surface of the parietal bone near the edge around the defect in weeks 2 and 3 (Figure 6a). The repaired bone was lined by cuboidal osteoblasts. The defect was not completely filled with the bone and the unrepaired defect was left with fibrous connective tissues in week 24 (Figure 6b). The repaired bone was lined by bone lining cells.

In situ *hybridization*
Defects 3.8 mm in diameter
Osteoblasts on the outer and inner bone surfaces near the edge around the defect and osteocytes nearby expressed type I collagen (Figure 7a) and osteocalcin (Figure 7b) in weeks 2 and 3. Osteoblasts and osteocytes that comprised the repairing bone projection also expressed type I collagen and osteocalcin. Osteoblasts expressing type I collagen and osteocalcin were

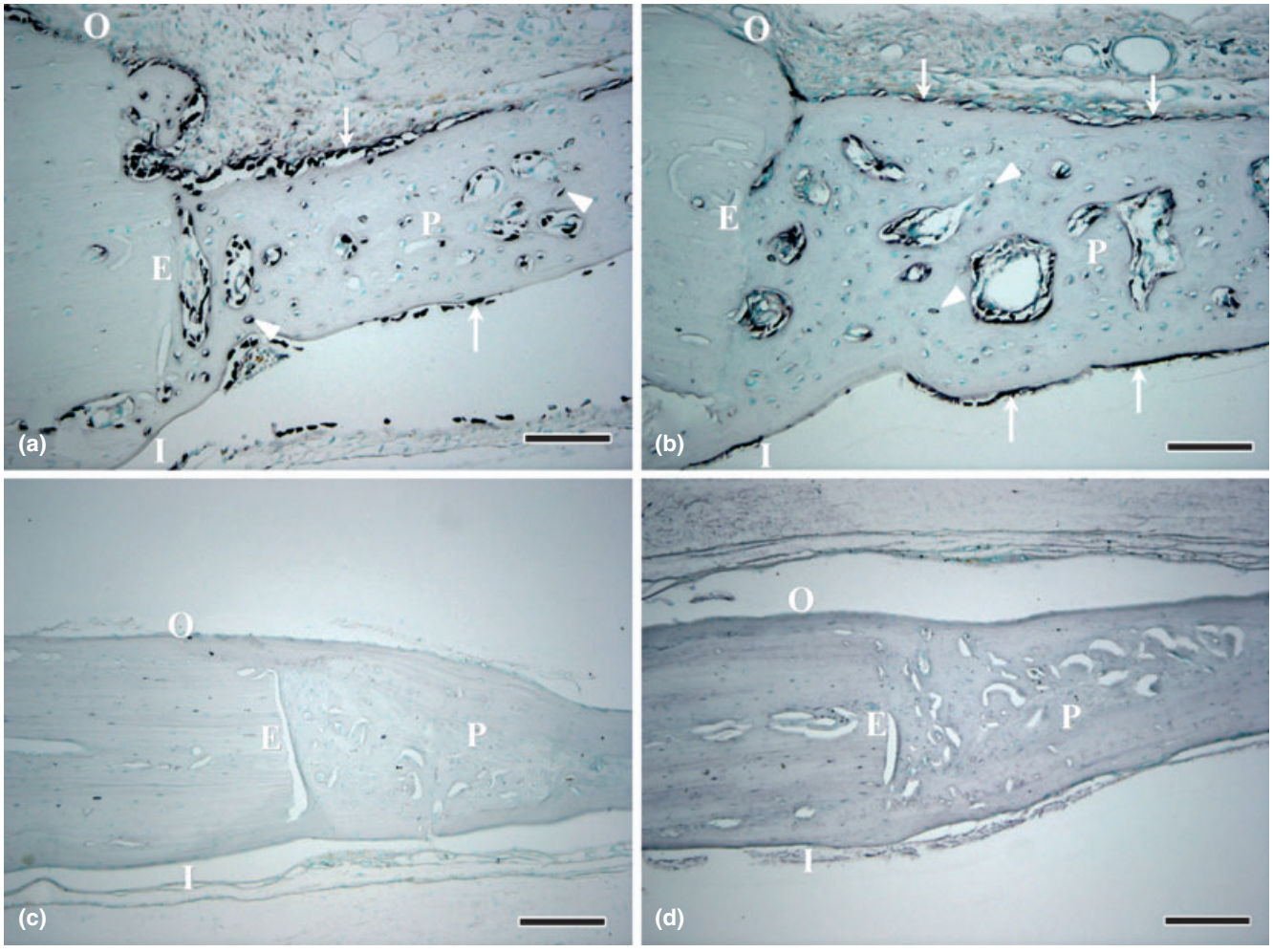

Figure 7 *In situ* hybridization for bone repair in 3.8 mm defects. Osteoblasts (arrows) on the outer (O) and the inner (I) bone surfaces near the edge (E) of the original defect and the repairing bone projection (P) as well as some osteocytes (arrowheads) in the bone matrix show strong signals for type I collagen (**a**) and osteocalcin (**b**) in week 3. Osteoblasts expressing type I collagen and osteocalcin are not identified on the surface of the bony edge (E) around the original defect. Expression of type I collagen (**c**) and osteocalcin (**d**) is no longer identified in repaired bone in week 24. Scale bars = 100 μm (**a**, **b**) and 200 μm (**c**, **d**)

not identified on the surface of the bony edge around the original bone defect. Expression of type I collagen (Figure 7c) and osteocalcin (Figure 7d) was no longer identified in repaired bone in week 24.

Defects 8.8 mm in diameter

Osteoblasts on the outer and inner bone surfaces near the edge around the defect and osteocytes nearby expressed type I collagen (Figure 8a) and osteocalcin

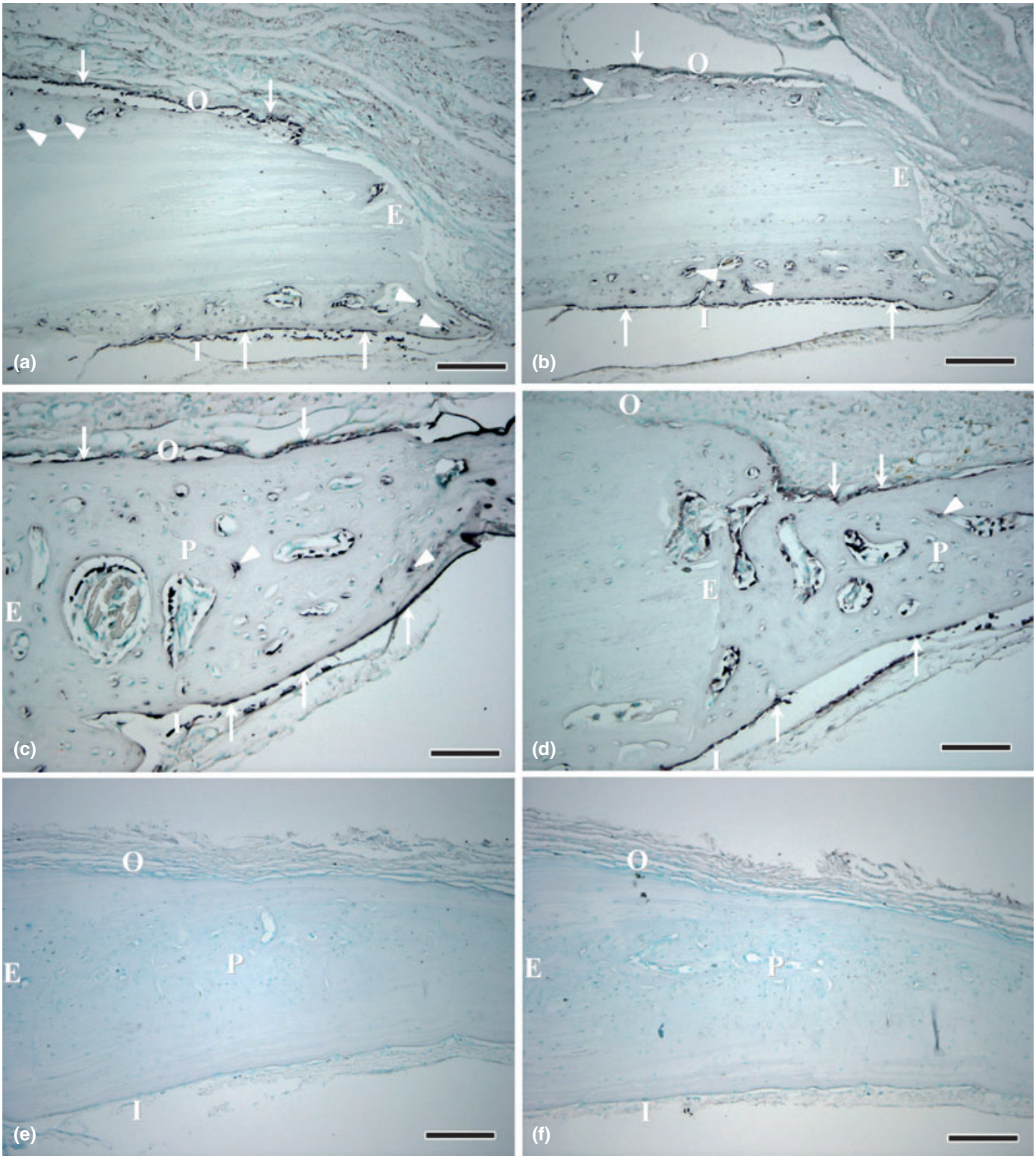

Figure 8 *In situ* hybridization for bone repair in 8.8 mm defects. Osteoblasts (arrows) on the outer (O) and inner (I) bone surfaces near the edge (E) of the defect and osteocytes (arrowheads) nearby show strong signals of type I collagen (**a**) and osteocalcin (**b**) in week 2. Osteoblasts and osteocytes in the bone projection (P) also express type I collagen (**c**) and osteocalcin (**d**) in week 3. Osteoblasts expressing type I collagen and osteocalcin are not identified on the surface of the bony edge (E) around the original defect. Expression of type I collagen (**e**) and osteocalcin (**f**) is no longer identified in the projection (P) of repaired bone in week 24. Scale bars = 200 μm (**a**, **b**, **e**, **f**) and 100 μm (**c**, **d**)

(Figure 8b) intensely in weeks 2 and 3. Osteoblasts and osteocytes in the bone projection also expressed type I collagen (Figure 8c) and osteocalcin (Figure 8d). Osteoblasts expressing type I collagen and osteocalcin were not identified on the surface of the bony edge around the original bone defect. Expression of type I collagen (Figure 8e) and osteocalcin (Figure 8f) was no longer identified in repaired bone in week 24.

Controls

Little expression of type I collagen and osteocalcin was recognized in the control parietal bone without any defect in 13-, 24- and 36-week-old rats.

Discussion

X-ray morphometry showed that formation of new bone in both large and small defects almost ceases within 24 weeks. A small defect is completely filled with bone by then, while the large bone defect is unrepaired and becomes a non-union with some fibrous connective tissues left in the unrepaired region. ISH showed that in week 24, bone lining cells on the surface of the new bone and osteocytes in the bone matrix express or produce little type I collagen and osteocalcin, which are major extracellular matrix (ECM) constituents in bone (Sasano *et al*, 2000; Zhu *et al*, 2001; Robey and Boskey, 2006). This suggests that bone formation by osteoblasts in both small and large defects is quiescent in week 24, while osteoblasts on the repaired bone and osteocytes nearby produce these ECM molecules and form bone actively in weeks 2 and 3.

The radiograph analysis showed that the amount of repaired bone formed per week is the greatest in the fourth week and decreases thereafter in both small and large defects. It suggests that the time course of formation of repaired bone may be similar in small and large defects. The ISH data showed corresponding features in the production of bone ECM molecules in both defects, i.e. osteoblasts and osteocytes produce type I collagen and osteocalcin actively in weeks 2 and 3 but very little in week 24. Osteoblasts and osteocytes may cease bone formation and new osteoblasts may no longer be differentiated at 24 weeks regardless of completion of the defect repair. What makes osteoblasts or osteocytes cease production of the ECM molecules or progenitor cells stop differentiating into osteoblasts remains unknown.

It has been suggested that inflammation promotes osteoblast differentiation directly or indirectly (Rifas *et al*, 2003; Gortz *et al*, 2004; Shen *et al*, 2005). Inflammation caused by the surgical procedure may have initiated differentiation of osteoblasts in the present study. Meanwhile, the functional activity of osteoblasts and the potential of progenitor cells for differentiation to osteoblasts may decline as the inflammation calms down. Involvement of inflammation in the osteoblast activity and the differentiation may largely decrease within 24 weeks. Further studies are required for understanding how inflammation may regulate the functional activity of osteoblasts and the differentiation potential of the progenitor cells.

Periosteal cells contain subsets of progenitor cells that possess the potential to differentiate to osteoblasts. They are activated to produce new bone by physical and chemical stimulation, such as bone fracture, inflammation and tumour development (Wlodarski, 1989; Nakase *et al*, 1994; Jacobsen, 1997; Shimizu *et al*, 2001). In our study, bone repair proceeded from the periosteum on the outer and inner surfaces near the defect and not from the surface of the bony edge around the original defect. Osteoblasts and their progenitors residing in the periosteum of both sides participated in forming the projection of the regenerated bone. The study showed first that bone repair proceeds from the periosteum near the defect and not from the surface of the edge around the original bone defect. How the repaired bone is connected to the original bony edge surface remains unknown. Electron microscopy may give further structural information about the interface between the repaired bone and the bony edge surface. Bone formation was more noticeable on the inner surface of the periosteum than the upper surface. The inner, or dural, side may have been harmed less than the outer periosteum by the surgical procedure. Alternatively, the periosteum on the dural side may possess distinctive characteristics compared to the outer periosteum.

We propose that the formation of repaired bone ceases within 24 weeks in both critical-size and non-critical-size calvarial bone defects, regardless of completion of the defect repair. It is also suggested that osteoblasts and osteocytes cease bone formation, and differentiation of osteoblast progenitors declines in 24 weeks for both defects. Furthermore, bone repair proceeds from the periosteum on both sides of the parietal bone and not from the surface of the bony edge around the original defect. Further research will be required to elucidate the mechanism of imperfect repair of a critical-size bone defect. These results could provide useful information to develop new treatment of large bone defects.

Acknowledgements

This work was supported in part by grants-in-aid (15390550, 17659573 and 18890027) from the Ministry of Education, Science, Sports and Culture of Japan. We wish to thank Masami Eguchi and Yasuto Mikami, Division of Craniofacial Development and Regeneration, Tohoku University Graduate School of Dentistry, for their excellent assistance in this study.

References

Alsberg E, Hill EE, Mooney DJ (2001). Craniofacial tissue engineering. *Crit Rev Oral Biol Med* **12:** 64–75.

Blanquaert F, Saffar JL, Colombier ML, Carpentier G, Barritault D, Caruelle JP (1995). Heparan-like molecules induce the repair of skull defects. *Bone* **17:** 499–506.

Cowan CM, Shi YY, Aalami OO *et al* (2004). Adipose-derived adult stromal cells heal critical-size mouse calvarial defects. *Nat Biotechnol* **22:** 560–567.

Dimitriou R, Tsiridis E, Giannoudis PV (2005). Current concepts of molecular aspects of bone healing. *J Care Injured* **36:** 1392–1404.

Einhorn TA (2005). The science of fracture healing. *J Orthop Trauma* **19** (Suppl.)**:** S4–S6.

Gortz B, Hayer S, Redlich K *et al* (2004). Arthritis induces lymphocytic bone marrow inflammation and endosteal bone formation. *J Bone Miner Res* **19:** 990–998.

Jacobsen FS (1997). Periosteum: its relation to pediatric fractures. *J Pediatr Orthop B* **6:** 84–90.

Kamakura S, Sasano Y, Homma H, Suzuki O, Kagayama M, Motegi K (1999). Implantation of octacalcium phosphate(OCP) in rat skull defects enhances bone repair. *J Dent Res* **78:** 1682–1687.

Kamakura S, Sasano Y, Nakajo S *et al* (2001). Implantation of octacalcium phosphate combined with transforming growth factor-β1 enhances bone repair as well as resorption of the implant in rat skull defects. *J Biomed Mater Res* **57:** 175–182.

Kamakura S, Sasano Y, Shimizu T *et al* (2002). Implanted octacalcium phosphate is more resorbable than β-tricalcium phosphate and hydroxyapatite. *J Biomed Mater Res* **59:** 29–34.

Kamakura S, Nakajo S, Suzuki O, Sasano Y (2004). New scaffold for recombinant human bone morphogenetic protein-2. *J Biomed Mater Res A* **171:** 229–307.

Kamakura S, Sasaki K, Honda Y, Anada T, Suzuki O (2006). Octacalcium phosphate combined with collagen orthotopically enhances bone regeneration. *J Biomed Mater Res B* **79:** 210–217.

Lutolf MP, Weber FE, Schmoekel HG *et al* (2003). Repair of bone defects using synthetic mimetics of collagenous extracellular matrices. *Nat Biotechnol* **21:** 506–508.

Nakamura M, Sone S, Takahashi I, Mizoguchi I, Echigo S, Sasano Y (2005). Expression of versican and ADAMTS1,4, and 5 during bone development in the rat mandible and hind limb. *J Histochem Cytochem* **53:** 1553–1562.

Nakase T, Nomura S, Yoshikawa H *et al* (1994). Transient and localized expression of bone morphogenetic protein 4 messenger RNA during fracture healing. *J Bone Miner Res* **9:** 651–659.

Petite H, Viateau V, Bensaid W *et al* (2000). Tissue-engineered bone regeneration. *Nat Biotechnol* **18:** 959–963.

Precious DS, Hall BK (1994). Repair of fractured membrane bones. In: Hall BK, ed. *Bone, vol. 9. Differentiation and morphogenesis of bone*. CRC Press: Boca Raton, pp. 145–163.

Rifas L, Arackal S, Weitamann N (2003). Inflammatory T cells rapidly induce differentiation of human bone marrow stromal cells into mature osteoblasts. *J Cell Biochem* **88:** 650–659.

Robey PG, Boskey AL (2006). Extracellular matrix and biomineralization of bone. In: Favus MJ ed. *Primer on the metabolic bone diseases and disorders of mineral metabolism* 6th ed. American Society for Bone and Mineral Research: Washington, DC, pp. 12–19.

Sasano Y, Zhu JX, Kamakura S, Kusunoki S, Mizoguchi I, Kagayama M (2000). Expression of major bone extracellular matrix proteins during embryonic osteogenesis in rat mandibles. *Anat Embryol* **202:** 31–37.

Sasano Y, Maruya Y, Sato H *et al* (2001). Distinctive expression of extracellular matrix molecules at mRNA and protein levels during formation of cellular and acellular cementum in the rat. *Histochem J* **33:** 91–99.

Sasano Y, Zhu JX, Tsubota M *et al* (2002). Gene expression of MMP8 and MMP13 during embryonic development of bone and cartilage in the rat mandible and hind limb. *J Histochem Cytochem* **50:** 325–332.

Schmitz JP, Hollinger JO (1986). The critical size defect as an experimental model for craniomandibulofacial nonunions. *Clin Orthopaed Related Res* **205:** 299–308.

Schmitz JP, Schwartz Z, Hollinger JO, Boyan BD (1990). Characterization of rat calvarial nonunion defects. *Acta Anat* **138:** 185–192.

Shen F, Ruddy MJ, Plamondon P, Gaffen L (2005). Cytokines link osteoblasts and of interleukin-17- and TNF-α-induced genes in bone cells. *J Leukoc Biol* **77:** 388–399.

Shimizu T, Sasano Y, Nakajo S, Kagayama M, Shimauchi H (2001). Osteoblastic differentiation of periosteum-derived cells is promoted by the physical contact with the bone matrix in vivo. *Anat Rec* **264:** 72–81.

Wlodarski KH (1989). Normal and heterotopic periosteum. *Clin Orthop* **241:** 265–277.

Zhu JX, Sasano Y, Takahashi I, Mizogichi I, Kagayama M (2001). Temporal and spatial gene expression of major bone extracellular matrix molecules during embryonic mandibular osteogenesis in rats. *Histochem J* **33:** 25–35.